Effects of CSF Cut-off Pressure and Skull Flexure on Blast Induced Traumatic Brain Injury

Xiancheng Yu[1], David J. Sharp[2], and Mazdak Ghajari[1]
[1]Dyson School of Design Engineering, Imperial College London; [2]Division of Brain Sciences, Imperial College London

ABSTRACT

Mechanisms of blast induced traumatic brain injury (b
TBI), particularly the role of primary pressure wave, are still not fully understood. Recent neuropathological analyses of brain tissue from post-mortem cases of blast TBI indicate that the brain tissue close to ventricles sustains damage. Two possible explanations for this location of injury are CSF cut-off pressure effect and skull flexure effect. Here we investigate whether CSF cut-off pressure and/or skull flexure can produce large strain and strain rate concentrations at the CSF/brain interface. To test this hypothesis, a two-dimensional human head FE model of blast TBI is developed, composed of skin, skull, CSF, brain and ventricles. To model CSF volumetric response under negative pressure, a cut-off pressure was defined in the material model. If the pressure drops below the cut-off value, it is reset to that value. The CSF cut-off pressure effect was investigated by comparing brain deformation of CSF material models with and without cut-off pressure. The effect of skull flexure was studied by increasing skull stiffness. Results shows that CSF cut-off pressure leads to strain discontinuity at the CSF/brain interface and elevated strain levels in brain. Similar effects can be seen for strain rate distribution, though the discontinuity is not as pronounced as for strain distribution. Increasing skull stiffness reduces the strain level within cranium, but it does not have a significant effect on strain distribution. Interestingly, increasing skull stiffness did not have a significant influence on the level and distribution of strain rate. In this study we used a 2D brain model, an approach adopted in previous literature, which is one of the limitations. We will extend the work by using 3D models. Our results suggest that blast pressure wave can cause CSF pressure dropping to cut-off pressure, which leads to strain concentration in the brain near ventricles and that skull flexure increase the level of strain. These results may have implications for novel ways to better prevent bTBI.

INTRODUCTION

In recent military conflicts, Traumatic Brain Injury (TBI) is becoming a prevalent injury, caused by blast waves, inertial loading and foreign impacts (Kulkarni, 2013). These loadings are usually generated by Improvised Explosive Devices (IEDs), which have been widely used in modern conflicts. TBI is traditionally divided into closed TBI, where the skull has no fracture, and penetrating TBI, where the skull is penetrated. Closed TBI is very common in both vehicle accidents and blast loading scenarios (Okie, 2005).

Currently, most of the literatures are focused on the impact induced TBI (iTBI) and this area has been extensively studied. Many animal and post-mortem human tests have been conducted in this field. In the impact scenarios, the acceleration and deceleration of the human head is the essential mechanism of TBI (Horgan, 2005), and there have been some popular injury criteria developed for iTBI (Rezaei, 2014). However, research on blast induced TBI (bTBI) is rather limited.

There are several studies that explore possible injury mechanisms of bTBI, which are well discussed in Rosenfeld, 2013. As illustrated in Figure 1, the mechanisms of bTBI are summarized as primary blast injury (1-9), secondary blast injury (10-12), tertiary blast injury (13) and quaternary blast injury (14). The primary blast injury includes local effect (1-7) and systemic effects (8, 9). However, the injury mechanisms and criteria for bTBI are still not well understood. It has been proved by some researchers that the injury mechanism for bTBI is quite different from iTBI (Cernak, 2001). The mechanism of blast induced TBI is quite complicated. There are many factors that may contribute to the brain injury in blast injuries.

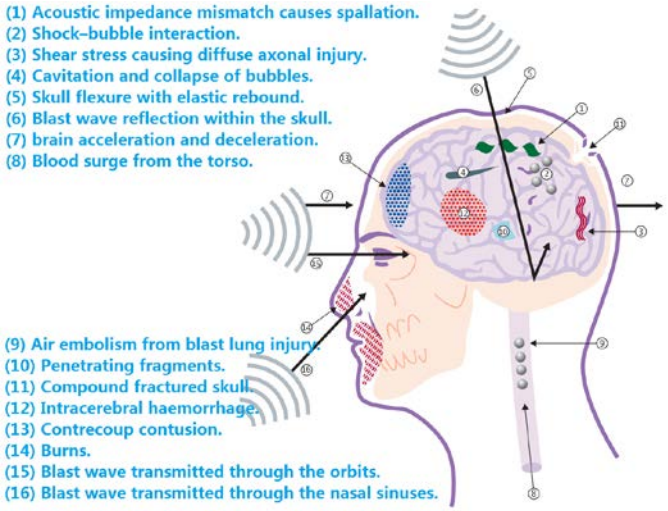

Figure 1: Mechanisms of blast induced TBI (Rosenfeld, 2013).

Recent neuropathological analyses of brain tissue from post-mortem cases of blast TBI show that the brain tissue close to ventricles sustains damage (Shively, 2016). This damage has not been seen in the civilian cases (impact TBI). This damage is likely to be produced by large loadings concentrated at the boundary of the brain and ventricles. Two possible explanations for

this location of injury are CSF cut-off pressure effect and skull flexure effect. The brain tissue and CSF have a very similar volumetric response under positive pressure, but CSF can only bear negative pressures up to its vapor pressure (-100 kPa), which usually refers to cut-off pressure (Goeller, 2012). CSF cut-off pressure can create a discontinuous pressure distribution, which may lead to strain concentration at its boundary with brain. Blast pressure wave can also generate skull flexure, causing brain deformations. In this paper, a two-dimensional human head model is developed to investigate whether CSF cut-off pressure and/or skull flexure can produce large strain and strain rate concentrations at the CSF/brain interface.

METHODS

A plane-strain FE human head model has been developed with LS-DYNA to explore the blast wave effect on human head (Figure 2). The geometry of the head model is based on an axial slice of a 3D head model, developed by Mazdak (Ghajari, 2016). The head is positioned in a blast domain. The Arbitrary Eulerian-Lagrangian (ALE) method is employed for the simulation of blast wave generation and fluid-structure interaction. All the simulations are ran for 2.1 ms. Based on this model, the two possible bTBI injury mechanism mechanisms are investigated.

It has been reported that FE models simulating blast loadings, generated by small charge weight (<1 kg TNT) and standoff distance (<1 m), may produce realistic peak overpressure but very short positive-phase duration (Chafi, 2010; Moore, 2009; Nyein,2010) compared with the real open field blast loading scenarios. The choices of the charge weight and standoff distance in these simulations are restricted due to the computational costs and the model dimension. Thus, the positive-phase duration in the simulations are relatively short. In all the simulations, the positive-phase duration of the blast wave is 0.2 ms and the incident overpressures are 12.5 bar. This loading is the lung damage threshold of a 70-kg male, subjected to free-field blast (Bowen, 1968).

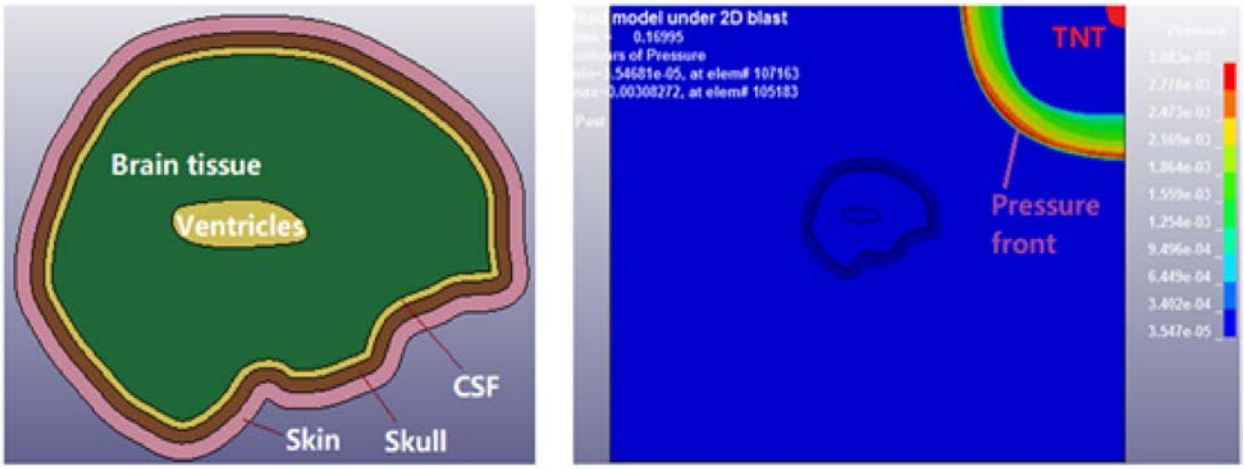

Figure 2: 2D human head FE model and blast loading generation.

The head components in the model are simplified as scalp, skull, CSF and brain tissue. Their material properties are listed in Table 1. The deviatoric response of the scalp, skull and brain

tissue is modelled with a linear viscoelastic model. The deviatoric response of CSF is represented by the dynamic viscosity at body temperature. The volumetric response of CSF was modelled using the Gruneisen equation of state, shown below, with the properties of water:

$$P = \rho_0 C^2 \mu \frac{1-(1-\gamma/2)\mu}{[1-(S_1-1)\mu]^2} \quad \text{for } \mu > 0 \text{ (Compression)}$$
$$P = \rho_0 C^2 \mu \quad \text{for } \mu < 0 \text{ (Tension)}$$

The volumetric response of the scalp, skull and brain tissue were modelled by defining a bulk modulus. LS-DYNA does not accept an equation of state when using MAT_GENERAL_VISCOELASTIC to model these materials. Panzer, 2012 developed a user defined material in LS-DYNA to incorporate the volumetric response of scalp, skull and brain. In their user-defined material, they used Gruneisen EOS. To test whether a nonlinear EOS is required under typical blast wave pressure, the Gruneisen EOS with their material properties was plotted as well as the linear EOS used in current study (Figure 3). As can be seen in this figure, the volumetric behavior is almost linear up to pressures well beyond those predicted within the brain under typical blast wave pressures (<2 MPa), which can be represented by simply defining a bulk modulus.

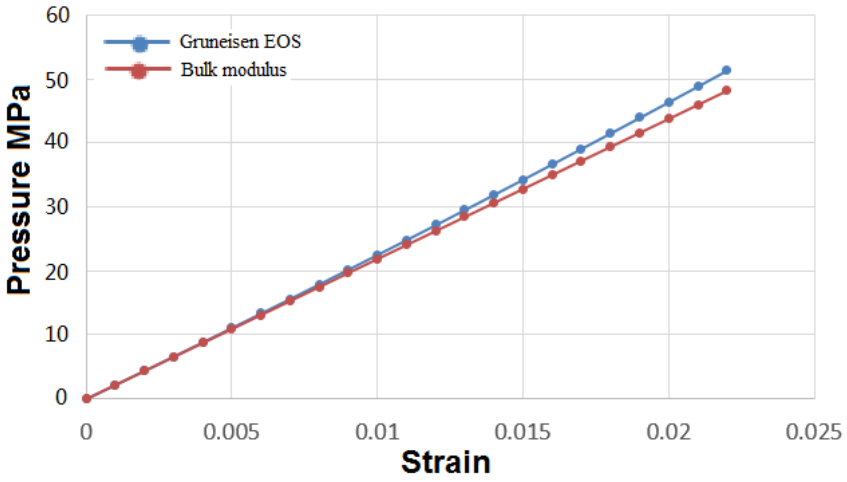

Figure. 3 The comparison of volumetric response (under compression) between Gruneisen EOS and bulk modulus

The CSF cavitation behavior was modelled by defining the cut-off pressure (Schiffer, 2017 and Panzer, 2012). Once the pressure of an element reaches the cut-off pressure, the element can expand without decrease of pressure. There are some different cavitation pressures used in various literatures. Here, the cut-off pressure is set to -100 kPa, according to Klug, 2013.

Table 1: Lists of acoustic of different materials (Panzer, 2012)

Materials	Bulk properties		Shear properties	
Scalp	$\rho = 1.13$ g/cm^3	$K = 2189$ MPa	$G_1 = 355$ kPa $G_2 = 399$ kPa $G_3 = 35.6$ kPa $G_\infty = 408$ kPa	$\beta_1 = 0.005$ ms^{-1} $\beta_2 = 0.05$ ms^{-1} $\beta_3 = 0.5$ ms^{-1}
Skull	$\rho = 2.00$ g/cm^3	$K = 10227$ MPa	$G_1 = 2289.6$ kPa $G_2 = 4708.5$ kPa $G_\infty = 4720.3$ kPa	$\beta_1 = 0.03$ ms^{-1} $\beta_2 = 275$ ms^{-1}
CSF	$\rho = 1.00$ g/cm^3 $C = 1484$ m/s $S_1 = 1.979$	$\Gamma_0 = 0.110$ $P_{cav} = -100$ kPa	$\mu = 8 \times 10^{-4}$ Pa s	
Brain	$\rho = 1.06$ g/cm^3	$K = 2188$ MPa	$G_1 = 50$ kPa $G_2 = 6.124$ kPa $G_3 = 2.496$ kPa $G_4 = 1.228$ kPa $G_5 = 1.618$ kPa $G\infty = 0.27$ kPa	$\beta_1 = 100$ ms^{-1} $\beta_2 = 4.35$ ms^{-1} $\beta_3 = 0.2$ ms^{-1} $\beta_4 = 0.0053$ ms^{-1} $\beta_5 = 5.1\times10^{-6}$ ms^{-1}

Skull flexure has also been reported to be a main factor that causes brain injury (Moss, 2009), but the previous simulations cannot distinguish the effect of skull flexure and cavitation. The skull flexure effect is studied by changing the skull stiffness and comparing the brain strain contours. Two simulations are conducted. In both simulations, the CSF is modelled with cavitation behavior, but in one the normal skull material is used and in the other simulation the skull stiffness is increased 5 times to decrease the effect of skull flexure.

RESULTS

Cut-off pressure effect

The CSF cut-off pressure effect was identified by comparing brain deformation of CSF material models with and without cut-off pressure. The first principal Green-Lagrange strain and strain rate (called strain and strain rate hereafter) contours are shown in Figure 4. Figure 4(a) shows the strain distribution of brain, using CSF material model without cut-off pressure. There is no strain concentration in the brain tissue around the ventricles. However, when cut-off pressure is included in the CSF model, clear concentration of strain in brain is observed, as illustrated in Figure 4(b). Similar results are also indicated in strain rate contour. Figure 5 indicates that CSF cut-off pressure also contributes to the increase in strain rate in the brain near the ventricles.

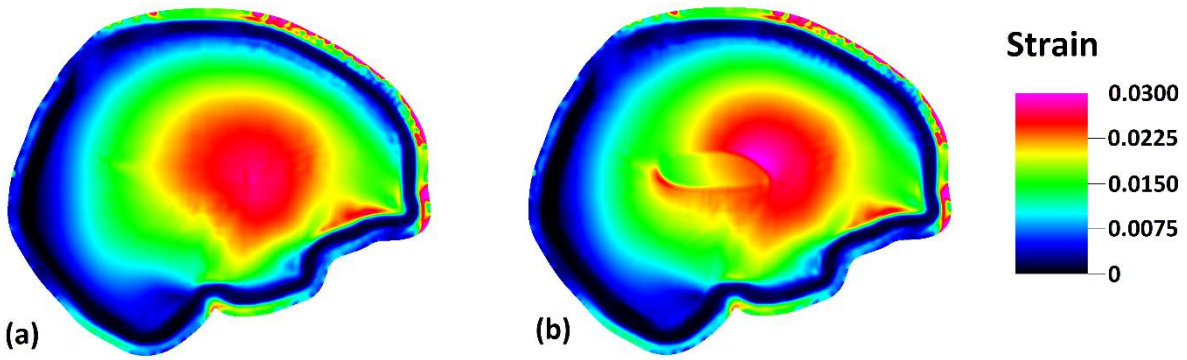

Figure 4: Strain distribution of brain tissue, using CSF models (a) without cut-off pressure and (b) with cut-off pressure.

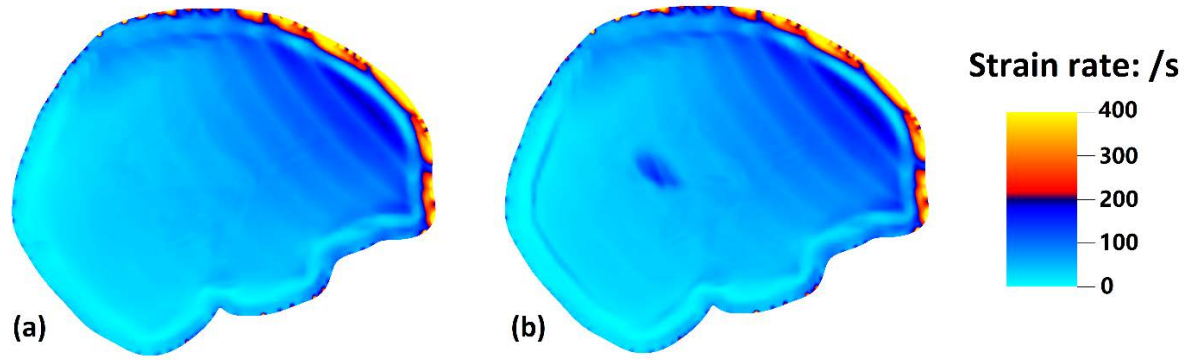

Figure 5: Strain rate distribution of brain tissue, using CSF models (a) without cut-off pressure and (b) with cut-off pressure.

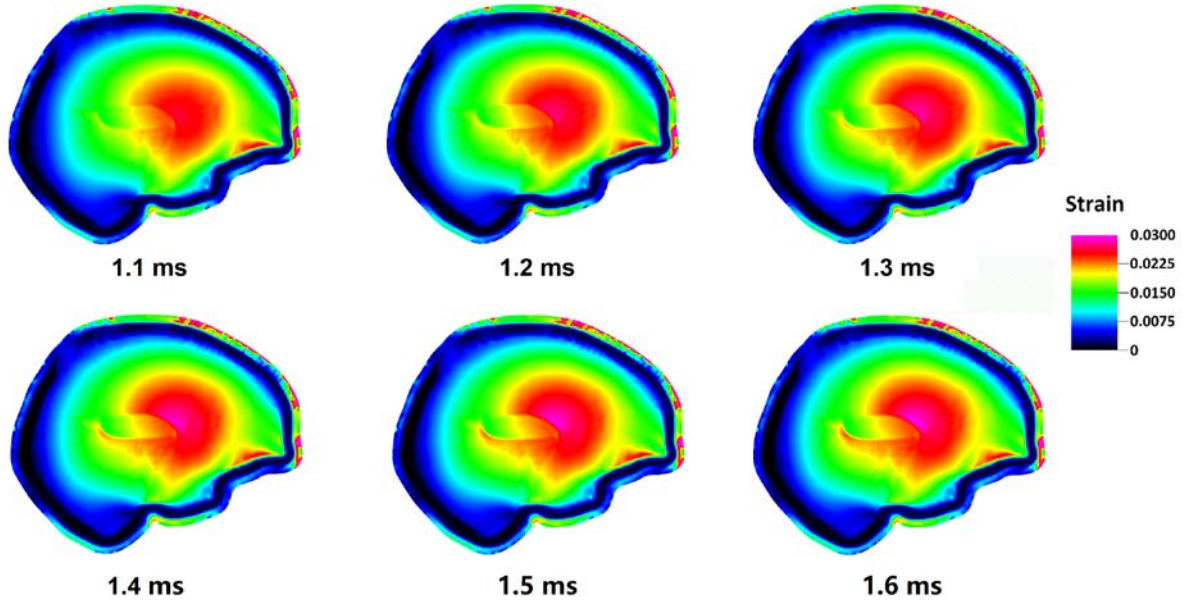

Figure 6: History of strain in brain tissue of simulation with cut-off pressure

Figure 6 shows the time history of the strain distribution of simulation with cut-off pressure. It shows that the strain concentration in brain increases gradually. This is because the shock wave transmits and reflects within the head many times. Cavitation will occur each time when a tensile wave passes the CSF and reaches the cavitation pressure. Correspondingly, the strain concentration increases each time a cavitation occurs. Thus, on the strain contour, the concentration phenomenon increases with time.

Skull flexure effect

Figure 7 shows the strain distribution of brain with a 5 times stiffer skull. Figure 4(b) and Figure 7(a) have the same strain contour range (0-0.03). Figure 7(a) has a lower overall strain level than Figure 4(b). This comparison shows that the skull flexure is an important factor to the overall strain level in the brain. Stiffer skull can reduce the overall strain level because of smaller deformation. But when the range is reduced to 0-0.02 (Figure 7(b)), the strain concentration in the brain tissues near the ventricle becomes obvious. This shows again that the cavitation of CSF contributes to the strain concentration of surrounding brain tissue. Figure 8 shows the strain rate distribution of brain with 5 times stiffer skull. There is no significant change, comparing with a normal skull (Figure 5(b)).

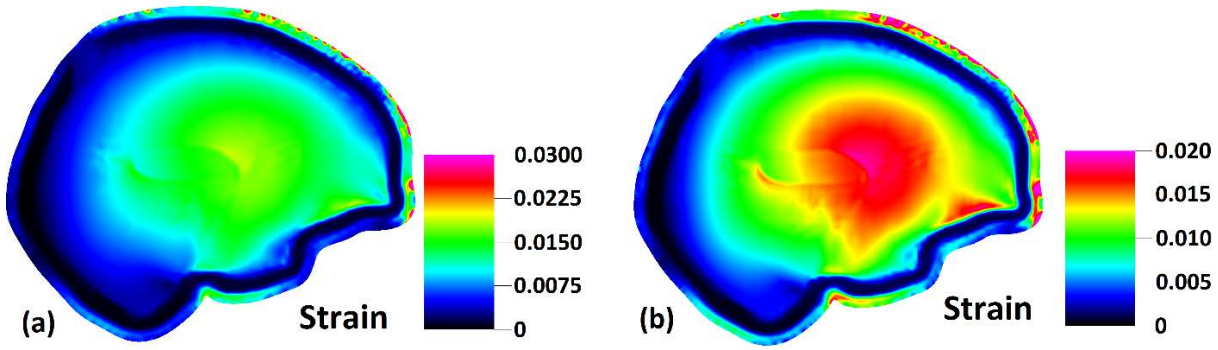

Figure 7: Strain distribution of brain with 5 times stiffer skull (a) strain contour range: 0-0.03 and (b) strain contour range: 0-0.02.

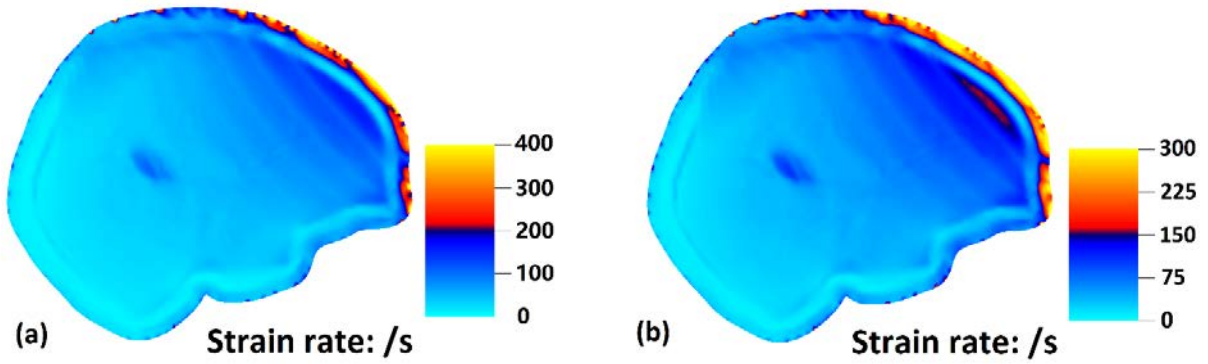

Figure 8: Strain rate distribution of brain with 5 times stiffer skull (a) strain rate contour range: 0-400 /s and (b) strain contour range: 0-300 /s.

CONCLUSIONS

CSF volumetric response contributes to the strain and strain rate concentration in the brain tissue near the ventricles. This effect is caused by the CSF element volumetric stiffness reducing to zero when reaching cavitation pressure, which means the pressure of CSF element continues to decrease with the expansion of the element. This created a discontinuous effect on the nearby brain tissue and cause strain/strain rate concentration.

Skull flexure can increase the overall deformation of brain tissue because of the compression on the internal brain tissue. Increasing skull stiffness reduces the strain level within cranium, but it does not have a significant effect on strain distribution. Interestingly, increasing skull stiffness did not have a significant influence on the level and distribution of strain rate.

In this study we used a 2D brain model, an approach adopted in previous literature (Panzer, 2012), which is one of the limitations. We will extend the work by using 3D models.

ACKNOWLEDGEMENTS

This work was conducted under the auspices of the Royal British Legion Centre for Blast Injury Studies at Imperial College London. The authors would like to acknowledge the financial support of the Royal British Legion.

REFERENCES

Kulkarni SG, Gao XL, Horner SE, Zheng JQ, David NV. Ballistic helmets – their design, materials, and performance against traumatic brain injury. Compos Struct 2013;101:313–31.

Okie, S., 2005. Traumatic brain injury in the war zone. New England Journal of Medicine, 352(20), pp.2043-2047.D. L. McArthur, D. J. Chute, and J. P. Villablanca, Brain Pathology 14, 185 (2004).

Rezaei, A., Karami, G. and Ziejewski, M., 2014. Examination of brain Injury thresholds in terms of the severity of head motion and the brain stresses. Intern Neurotrauma Lett, 35.

Rosenfeld, J. V., McFarlane, A. C., Bragge, P., Armonda, R. A., Grimes, J. B., & Ling, G. S. (2013). Blast-related traumatic brain injury. The Lancet Neurology, 12(9), 882-893.

Cernak, I.; Wang, Z.; Jiang, J.; Bian, X.; Savic, J. The Journal of trauma 2001, 50, 695-706.

Shively, S.B., Horkayne-Szakaly, I., Jones, R.V., Kelly, J.P., Armstrong, R.C. and Perl, D.P., 2016. Characterisation of interface astroglial scarring in the human brain after blast exposure: a post-mortem case series. The Lancet Neurology, 15(9), pp.944-953.

Goeller, J., Wardlaw, A., Treichler, D., O'Bruba, J. and Weiss, G., 2012. Investigation of cavitation as a possible damage mechanism in blast-induced traumatic brain injury. Journal of neurotrauma, 29(10), pp.1970-1981.

Ghajari, M., Hellyer, P.J. and Sharp, D.J., 2016. Computational modelling of traumatic brain injury predicts the location of chronic traumatic encephalopathy pathology. Brain, p.aww317.

Chafi, M., G. Karami, and M. Ziejewski. Biomechanical assessment of brain dynamic responses due to blast pressure waves. Ann. Biomed. Eng. 38:490 – 504, 2010.

Moore, D. F., A. Jerusalem, M. Nyein, L. Noels, et al. Computational biology—modeling of primary blast effects on the central nervous system. Neuroimage. 47:T10 – T20, 2009.

Nyein, M. K., Jason, A. M., Yu, L., Pita, C. M., Joannopoulos, J. D., & Moore, D. F., et al. (2010). In silico investigation of intracranial blast mitigation with relevance to military traumatic brain injury. Proceedings of the National Academy of Sciences of the United States of America, 107(48), 402-424.

Bowen, I.G., Fletcher, E.R. and Richmond, D.R., 1968. Estimate of man's tolerance to the direct effects of air blast. LOVELACE FOUNDATION FOR MEDICAL EDUCATION AND RESEARCH ALBUQUERQUE NM.

Panzer, M.B., Myers, B.S., Capehart, B.P. and Bass, C.R., 2012. Development of a finite element model for blast brain injury and the effects of CSF cavitation. Annals of biomedical engineering, 40(7), pp.1530-1544.

Schiffer, A. and Tagarielli, V.L., 2017. Underwater blast loading of water-backed sandwich plates with elastic cores: Theoretical modelling and simulations. International Journal of Impact Engineering, 102, pp.62-73.

Moss, W.C., King, M.J. and Blackman, E.G., 2009. Skull flexure from blast waves: a mechanism for brain injury with implications for helmet design. Physical review letters, 103(10), p.108702.